Food Chemistry: X 14 (2022) 100340

Contents lists available at ScienceDirect

Food Chemistry: X

journal homepage: www.sciencedirect.com/journal/food-chemistry-x

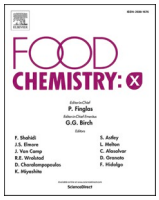

Physicochemical properties, structure, and ameliorative effects of insoluble dietary fiber from tea on slow transit constipation

Xiaoli Bai [a,b,1], Yi He [b,1], Bingyan Quan [a], Ting Xia [a], Xianglong Zhang [a], Yongqi Wang [a], Yu Zheng [a,*], Min Wang [a,*]

[a] State Key Laboratory of Food Nutrition and Safety, Key Laboratory of Industrial Fermentation Microbiology, College of Biotechnology, Tianjin University of Science and Technology, Tianjin 300457, China
[b] State Key Laboratory of Core Technology in Innovative Chinese Medicine, Tasly Pharmaceutical Group Co., Ltd, Tianjin 300410, China

ARTICLE INFO

Keywords:
Tea
Insoluble dietary fiber
Physicochemical property
Slow transit constipation
In vitro fermentation

ABSTRACT

Tea residue is a by-product of tea processing and contains ~ 60 % insoluble dietary fiber. We investigated the physicochemical properties and structure of the insoluble dietary fiber of tea (T-IDF), and its defecation function was evaluated. The physical and chemical indexes of the T-IDF, including its water holding, oil holding, swelling, cation exchange, and cholesterol exchange capacities, were measured, while its structure was analyzed by a range of analytical techniques. Furthermore, the related indexes of the animal defecation function were determined, and the in vitro detection of fermented short chain fatty acid was conducted. We found that T-IDF exhibits excellent physical and chemical properties. Moreover, the consumption of T-IDF significantly promoted defecation in slow transit intestinal dyskinesia mice and enhanced the production of short chain fatty acids. Overall, we demonstrated a good correlation between the physicochemical properties and the structure/function of T-IDF.

1. Introduction

Dietary fiber (DF) is the general name given to indigestible carbohydrates and lignin, and it can be classified as either soluble dietary fiber (SDF) or insoluble dietary fiber (IDF). The main components of SDF are the stored substances and secretions of plant cells, in addition to certain microbial polysaccharides and synthetic polysaccharides. The structures of SDF the components generally display a high degree of branching; this is beneficial as it enables them to combine with harmful substances in the human intestine, where they are degraded into nutrients that are utilized by beneficial microorganisms (Bishehsari et al., 2018). The main components of IDF are cellulose, hemicellulose, lignin, and protopectin, which have compact structures and therefore cannot be used by intestinal microorganisms. Rather, their primary role is to promote intestinal peristalsis, which is immensely important for human health (Sacranie et al., 2012). Dose-response curves suggest that a high daily intake of DF between 25 and 29 g confers great health benefits by protecting against cardiovascular disease, type 2 diabetes, and breast and colorectal cancers. Unfortunately, the majority of individuals globally consume <20 g per day (Reynolds et al., 2019).

After water, tea is the most consumed drink worldwide, with the production and consumption of black tea being estimated to continue to increase over the next 10 years due to the strong demand for tea in developing and emerging countries (FAO, 2018). As a co-product of commercial black tea processing, tea fiber could be re-introduced into the food industry because it is rich in beneficial components such as DF, proteins, tea polyphenols, and tea polysaccharides (Tsubaki & Azuma, 2013).

Constipation is a common clinical problem that negatively affects the quality of life of many individuals globally. Based on a systematic review of the literature we found that the prevalence of constipation in the worldwide general population is very variable, ranging from 2.5 to 79 % in adults (Mugie, Benninga, & Di Lorenzo, 2011). Constipation can be divided into three categories, namely normal-transit constipation, defecatory or rectal evacuation disorders, and slow transit constipation (STC) (Zhang et al., 2018). Currently, anti-constipation medication is primarily used for the clinical treatment of constipation, with examples including Bisacodyl enteric-coated tablets, Tegaserod, Prucalopride,

* Corresponding authors.
E-mail addresses: yuzheng@tust.edu.cn (Y. Zheng), minw@tust.edu.cn (M. Wang).
[1] These authors contributed equally to this paper.

https://doi.org/10.1016/j.fochx.2022.100340
Received 25 December 2021; Received in revised form 8 May 2022; Accepted 18 May 2022
Available online 21 May 2022

Velusetrag, Lubiprostone, Linaclotide, and Plecanatide. Unfortunately, these medications can have serious side effects, and are generally costly. It has therefore been envisaged that natural, functional food materials that can prevent and relieve constipation by increasing the amount of fiber in the diet will have broad application in meeting human health needs.

Thus, we herein report the extraction of T-IDF from tea and subsequent investigation of its general properties, biochemical composition, and physicochemical characteristics. Using a constipation mouse model, the laxative properties of T-IDF are also investigated along with its effect on the small intestinal movements and the defecation process characteristics of T-IDF. Finally, the effects of T-IDF on the fermentation behavior in human fecal samples are examined by analyzing the degree of short-chain fatty acid production. In addition, the potential mechanism of T-IDF in ameliorating STC is also proposed. The novelty of our study lies in the fact that we report the systematic exploration of T-IDF to demonstrate its ability to enhance defecation. Furthermore, the determination of an effective dose is expected to provide a theoretical basis for its further development as a functional food.

2. Materials and methods

2.1. Materials

Pu-erh tea was provided by Yunnan Tasly Deepuer Biological Tea Group Co., ltd. (Pu'er city, China). The monosaccharide standards were purchased from Sigma-Aldrich (Shanghai, China), while the diphenoxylate tablets were obtained from Henan Dingchang Pharmaceutical Company (Jiaozuo, China). The Biantong capsules, which were used as the positive control, were obtained from the Wuhan Jianmin Pharmaceutical Company (Wuhan, China). All other chemicals used in the experiments were of analytical grade and were purchased from J&K Scientific ltd (Beijing, China).

2.2. Preparation of T-IDF

Water was used for the extraction process to effectively separate the water-soluble substances of Pu-erh tea from the insoluble substances, including the insoluble dietary fiber of the cell walls (i.e., T-IDF). More specifically, the Pu-erh tea sample was boiled in water (1:8, m/v) for 1 h, then filtered three times using a 300 mesh filter cloth. The filter residues were dried in an oven at 105 °C until the moisture content was <8 %, and then they were passed through an 80-mesh sieve and stored at 20 °C until required for analysis.

2.3. Composition analysis

2.3.1. Basic component analysis

The DF, IDF, and SDF contents were measured according to the AOAC method. The cellulose, hemicellulose, and lignin contents were determined according to the methods described by Van Soest et al. (Van Soest, Robertson, & Lewis, 1991). The proteins were analyzed according to the Kjeldahl method, the pectin content was measured by the method derived by Robertson (Robertson, 1979), and the fat content was determined using the AOAC method. Furthermore, the polyphenol content was determined using the Folin–Ciocalteu method (Waterhouse, 2003), and the polysaccharide content was determined according to the phenol–sulfuric acid method (Cuesta et al., 2003). The theabrownin content was determined by spectrophotometry. All experiments were performed in triplicate.

2.3.2. Monosaccharide compositional analysis

The monosaccharide composition was evaluated by acid hydrolysis and high-performance anion-exchange chromatography (HPAEC). The standard monosaccharides included fucose, rhamnose, arabinose, galactose, glucose, xylose, mannose, D-fructose, D-ribose, galacturonic acid, glucuronic acid, aminogalactose hydrochloride, glucosamine hydrochloride, *N*-acetyl-glucosamine, L-guluronic acid, and D-mannuronic acid.

2.3.3. Amino acid compositional analysis

The amino acid compositional analysis was carried out using pre-column derivatization reverse phase–high performance liquid chromatography (RP-HPLC) by means of acid hydrolysis, alkaline hydrolysis, oxidative acid hydrolysis, and derivatization with 2,4-dinitrofluorobenzene (Temtrirath, 2022).

Sample processing: Acid hydrolysis was performed by heating the samples at 110 °C in a 6 mol/L HCl solution for 22 h under anoxic conditions. Alkaline hydrolysis was performed by heating the samples at 110 °C in a 4 mol/L NaOH solution for 20 h under anoxic conditions. Oxidative acid hydrolysis was conducted at 0 °C in a performic acid solution (90:30, formic acid:hydrogen peroxide) for 16 h followed by hydrolysis in a 6 mol/L HCl solution at 110 °C for 24 h. 2,4-Dinitrofluorobenzene was used as the pre-column derivatization reagent, and derivatization was conducted under 60 °C for 1 h in the dark (Li, Liu, Zhao, Zheng, Lu, & Liang, 2016). Each sample was filtered through a 0.45 μm membrane filter prior to testing.

Chromatographic conditions: Instrument: Agilent 1100 high-performance liquid chromatograph equipped with a diode array detector; Chromatographic column: ZORBAX SB-C18 (4.6 × 250 mm × 5 μm); Flow rate: 1.0 mL/min; Detection wavelength: 360 nm; Column temperature: 36 °C; Sample volume 10 μL; Mobile phase: gradient elution with an aqueous sodium acetate solution (A, 0.04 mol/L, pH 6.30) and acetonitrile/water (B, 1:1, v/v). The solvent composition was varied as follows: 0–9 min, 70 % A; 9–15 min, 68 % A; 15–23 min, 55 % A; 23–28 min, 47 % A; 28–36 min, 41 % A; 36–47 % min, 14 % A; 47–49 min, 4 % A; and 49–53 min, 70 % A. The external standard method was used to calculate the concentration of each amino acid.

2.3.4. Mineral element compositional analysis

The mineral concentrations were measured according to the method described by Zhang (Zhang et al., 2017) using a flame atomic absorption spectrometer (Haiguang, GGX-910, China) equipped with single hollow-cathode lamps for each element, and an air acetylene burner. The mineral concentrations were quantified using calibration curves obtained using various standards. Each sample (0.5 g) was dissolved in a 1 mol/L hydrochloric acid(15 mL). Prior to analysis, the sample volume was then made up to 100 mL using distilled water. For the trace element measurements, the dried sample (0.5 g) was digested in a mixture of 37 % hydrochloric acid (5 mL) and 63 % nitric acid (10 mL), then diluted to 100 mL using distilled water.

2.4. Physicochemical properties

2.4.1. Water holding capacity

Each sample (0.5 g) was mixed thoroughly with distilled water (10 mL) at 20℃ for 12 h; the slurry was then centrifuged at 2800×*g* for 25 min and the supernatant was removed by slowly tilting the centrifuge tube (Luo et al., 2017). The water holding capacity (WHC) was calculated using the equation below:

$$\mathrm{WHC}\ (\mathrm{g/g}) = \mathrm{m_2/m_1}$$

where m_1 is the weight of the sample prior to hydration, and m_2 is the weight of the hydrated sample.

2.4.2. Oil holding capability

Each sample (0.5 g) was mixed thoroughly with soybean oil (4.0 g), sealed, and placed in a 37 °C water bath for 4 h; the slurry was then centrifuged at 2800×*g* for 15 min (Zhang et al., 2017). The oil holding capacity (OHC) was calculated using the equation below:

$$OHC\ (g/g) = m_2/m_1$$

where m_1 is the weight of the dried sample, and m_2 is the weight of the centrifuge tube containing the sample and the oil.

2.4.3. Swelling capacity

Each sample (0.250 g) was mixed thoroughly with distilled water (5 mL) in a graduated cylinder at 20℃ for 12 h (Luo et al., 2017). After this time, the swelling capacity (SC) was calculated using the equation:

$$SC\ (mL/g) = (V_1\text{-}V_0)/m_0$$

where V_0 is the volume of the dried sample, V_1 is the volume of the hydrated sample, and m_0 is the weight of the dried sample.

2.4.4. Cation exchange capability

Each sample (0.5 g) was suspended in a 0.1 mol/L hydrochloric acid solution (20 mL) at 20℃ for 12 h. After subsequent filtration, the residue was washed with distilled water to remove the chloride ions. Prior to titration with a 0.1 mol/L sodium hydroxide solution using 0.5 % phenolphthalein-ethanol solution as an indicator, the residue was dissolved in a 5 % sodium chloride solution (100 mL) and stirred for 30 min (Benitez, Molla, Martin-Cabrejas, Aguilera, & Esteban, 2017). The cation exchange capability (CEC) was calculated using the equation below:

$$Cation\ exchange\ capability/(mmoL/g) = (V_1 - V_0) \times 0.1/m$$

where V_1 is the volume of sodium hydroxide solution consumed by the titration sample in m_l, V_0 is the volume of sodium hydroxide solution consumed by the titration blank in m_l, m is the dry mass of the sample in g, and 0.1 is the concentration of the sodium hydroxide solution used for the titration in mol/L.

2.4.5. Cholesterol absorption capability

Egg yolk was whipped 9 times with distilled water to make an emulsion. Each sample (0.5 g) was mixed thoroughly with the egg yolk emulsion (25.0 g) at pH 2.0 (the stomach environment) and pH 7.0 (the small intestine environment) at 20℃. The obtained mixture in each case was then shaken at 37 °C for 2 h and subjected to centrifugation at 2800×*g* for 20 min. After this time, the supernatant (1.0 mL) was added to glacial hexanoic acid to achieve a final volume of 4.0 mL. The absorbance value was measured at 560 nm using the ferric ammonium sulfate color method (Luo et al., 2017), and the cholesterol absorption capability (CAC) was calculated using the equation below:

$$\text{Cholesterol absorption capability}(mg/g) = (m_2\text{-}m_1)/m$$

where m_2 is the cholesterol content in the egg yolk before adsorption (mg), m_1 is the cholesterol content in the supernatant after adsorption (mg), and m is the weight of DF (g).

2.5. Structural analysis

2.5.1. Scanning electron microscopy

Scanning electron microscopy (SEM) was conducted to analyze the micro-structure and surface characteristics of T-IDF (S-3000 N scanning electron microscope, Hitachi, Japan). Prior to analysis, the samples were sputter-coated with Au over a period of 180 s. SEM analysis was performed at an acceleration voltage of 5 kV using an SE2 detector (secondary electron detector), a working distance of 6.2 mm, and magnifications of 5000 and 10,000 times.

2.5.2. X-ray diffraction

The X-ray diffraction (XRD) measurements were carried out using a JDX-I0P 3A diffractometer (Japan Electron Optics Laboratory, Tokyo, Japan) with copper Kα radiation (0.1542 nm, 40 kV, and 50 mA) in the 2θ degree range of 5–70°. When lattice distortion was not considered, the Scherrer formula was used to calculate the grain size of the T-IDF, according to the formula below:

$$D = \frac{K.\lambda}{Bhkl.\cos\theta}$$

where D is the grain diameter along the direction perpendicular to the crystal plane, K is the Scherrer constant (K = 0.89 in this calculation), λ is the incident X-ray wavelength, Bhkl is the half-width of the diffraction peak, and θ is the Bragg diffraction angle (Yalcin et al., 2015).

2.5.3. Fourier transform infrared spectroscopy

Fourier transform infrared spectroscopy (FT-IR) was performed using a Tensor 27 infrared spectrometer (Bruker, Germany) according to the KBr disc method. More specifically, the dried sample (1 mg) was ground with KBr (100 mg, spectroscopic grade) and scanned with a blank KBr background. The sample spectra were collected with a resolution of 4 cm^{-1} over a wavenumber range of 4000–400 cm^{-1}. The FT-IR spectra were recorded in transmittance mode with a scan number of 32. The FT-IR spectral parameters of the samples were obtained and analyzed using the OMNIC FT-IR version 7.2a software package (Thermo Electron Corporation, USA) for baseline correction, smoothing, and peak calibration.

2.6. Animal experiments

2.6.1. Animals and the environment

Male BALB/c mice (6–8 weeks old, 20 ± 2 g) were purchased from Beijing Vital River Laboratory Animal Technology Co., ltd. (Beijing, China). The animal procedures were performed according to the guidelines of the Institutional Animal Ethics Committee and were approved by the Institutional Animal Committee of Nankai University. The animals were kept in a contained barrier animal room under standard conditions with a 12/12 h light–dark cycle at 20℃ and a relative humidity of 60 ± 5 % at the Institute of Pharmacology and Toxicology, Tasly Holding Group (Tianjin, China).

2.6.2. Grouping and dose design

After a one-week adaptive phase, 144 mice were randomly divided into two groups, each containing 72 mice each. Small intestinal movement tests and defecation tests were performed. Each group was split into 6 subgroups (n = 12), including the normal group, the model group (0.25 mg/mL diphenoxylate), the positive control group (14 mg/mL Biantong capsules), the T-IDF low dose group (1.7 g/kg T-IDF), the T-IDF middle dose group (3.3 g/kg T-IDF), and the T-IDF high dose group (6.7 g/kg T-IDF).

2.6.3. Animal experimental method

2.6.3.1. Method and time for sample administration. The mice in each group were administered the corresponding treatment by gavage (0.2 mL/10 g) twice daily for 14 d.

2.6.3.2. Establishment of a model. On the final day of the experiment, all animals were fasted for 16 h. The normal group was given distilled water, the groups undergoing the small intestinal movement test were administered diphenoxylate (5 mg/kg), and the defecation test groups were administered diphenoxylate (10 mg/kg).

2.6.3.3. Small intestinal movement tests. After the administration of diphenoxylate for 30 min, the positive control and dose groups were administered ink containing the corresponding treatment. The normal and model groups were administered ink by gavage. After a further 25 min, the mice were killed by cervical dislocation. The intestines, from the pylorus to the ileocecal valve, were removed by laparotomy. The length of the intestinal tube (i.e., the total intestine length) and the

length of ink from the pylorus to the foremost edge of the ink (i.e., the ink pushing length) were used to calculate the ink pushing rate according to the formula below (Ritz, Lin, Wilson, Barton, & Lin, 2017):

$$Ink\ pushing\ rate\ (\%) = \frac{ink\ pushing\ length}{total\ intestine\ length} \times 100$$

2.6.3.4. Defecation tests. After the administration of diphenoxylate for 30 min, the positive control and dose groups were administered ink containing the corresponding treatment. The normal and model groups were administered ink by gavage (Tadesse, Engidawork, Nedi, & Mengistu, 2017). The first dejection time, grain number, and the total weight of black feces produced within 6 h were recorded.

2.6.4. Evaluation standard

The defecation function is commonly evaluated based on the small intestinal movement and by defecation tests. For the purpose of this study, the evaluation method was determined based on the method of Liu et al. with minor modifications (Liu, Chen, Yan, Li, & Jiang, 2019). Compared with the normal group, the small intestine movement test or dejection time exhibited a positive result, and the feces weight or grain number exhibited a positive result. This could account for the positive results from the animal experiments on the laxative effects. This could account for the positive results resulting from the animal experiments determining the laxative effects of T-IDF treatment.

2.7. In vitro fermentation of T-IDF

2.7.1. Preparation of the human fecal inoculum

The inclusion criteria for the human fecal donors (n = 4) were as follows: age, 25–50 years old; sex, 50 % of the donors were female, 50 % were male; other criteria, non-smoking, non-vegetarian, normal defecation, no history of gastrointestinal disease, and no intake of antibiotics three months prior to donation (Breynaert et al., 2015). Each fecal sample (1 g) was diluted with peptone water (5 mL).

2.7.2. In vitro fermentation

The medium for the in vitro fermentation trial was prepared according to a previous study (Zhao, Nyman, & Jonsson, 2006). T-IDF and the medium were added into the human fecal inoculum, and then mixed in a 50 mL polypropylene centrifuge tube. The samples contained 4.5 mL medium, 4.5 mL fecal inoculum, and 1 mL T-IDF (50 mg/mL) or distilled water. The tubes were incubated at 37 ℃ and 200 rpm in a ZHWY-2102 Incubation Shaker (Zhi Cheng Corp., Shanghai, China) for 0, 6, 12, 24, 36, and 48 h.

2.7.3. Analysis of the short-chain fatty acids (SCFAs)

For quantification of the short chain fatty acids, calibration curves were initially established using the reference substances, and the quantitative results were obtained by comparison of the analyzed samples with these curves. The samples were placed into polypropylene tubes and centrifuged at 5000 rpm × g for 20 min, after which the supernatant was filtered through a 0.22 μm membrane filter (Millipore, MA, USA). The suspension was adjusted to pH 2.0 using a 5 mol/L HCl solution prior to analysis of the SCFA composition by gas chromatography (GC, Agilent 6890 N Agilent Technologies Corp., USA) with flame ionization detection (FID). The GC column (30 m × 0.53 mm × 1 μm) was an HP-FFAP column (19091F-413, Agilent Technologies Corp., USA). Nitrogen was used as the carrier gas at a flux rate of 3.0 mL/min with a split ratio of 1:20. The initial oven temperature was 100 ℃, which was maintained for 0.5 min, then increased to 180 ℃ at a rate of 10 ℃/min and maintained for 1 min. The temperature was then increased to 200 ℃ at a rate of 20 ℃/min and maintained for 5 min. The temperatures of the FID and the injection port were 240 and 200 ℃, respectively. The injected sample volume was 1 μL. Each sample was analyzed in triplicate.

2.8. Statistical analysis

All results are presented as the mean ± standard deviation. Comparisons among the whole groups were performed by one-way analysis of variance (ANOVA). Significant differences were analyzed according to the Bonferroni post hoc test. Statistical significance was observed when $p < 0.05$.

3. Results and discussion

3.1. Characterization of the T-IDF

3.1.1. Chemical composition

T-IDF is composed mainly of IDF and protein (60.40 and 22.86 %, respectively, 37.85 % protein–fiber index), followed by polyphenols (1.34 %), fats (1.20 %), polysaccharides (0.49 %), and theabrownin (0.34 %) (Fig. 1A). The cellulose, hemicellulose, and lignin contents of T-IDF were 13.60, 8, and 28.60 %, respectively. In addition, 5 % pectin was also detected in T-IDF. The high content of insoluble dietary fiber in the T-IDF sample indicates that it can absorb water, soften stools, and increase its volume to stimulate peristalsis and speed up defecation. In addition, it is known that cellulose tends to combine with hemicellulose, lignin, and pectin to influence the textures of plant-derived foods.

The monosaccharide composition of T-IDF was analyzed by HPAEC, whereby 8 monosaccharides were detected. More specifically, the 6 neutral monosaccharides detected in descending order were: xylose > galactose > glucose > arabinose > rhamnose > fucose, in a molar ratio of 0.370:0.234:0.163:0.142:0.019:0.016 (Fig. 1B). The high concentration of xylose in T-IDF may be related to its hemicellulose content. Small amounts of galacturonic acid (and acidic sugar) and glucosamine (and alkaline sugar) were also detected. We note that the T-IDF sample exhibited comprehensive advantages in terms of its amino acid and mineral nutritional values. More specifically, nineteen amino acids were detected in T-IDF (Table 1), including 8 essential amino acids and 11 non-essential amino acids. The ratio of the essential to non-essential amino acids was 0.90, which is higher than the 0.6 specified by the FAO/WHO standard. In addition, the essential amino acid content accounted for 47 % of the total amino acid content, which met the FAO/WHO standard. Furthermore, eighteen mineral elements were detected in T-IDF giving a total content of 5.15×10^4 mg/kg (Table 1); these elements are essential for maintaining human health, thereby indicating the suitability of T-IDF to be used as a food supplement. Indeed, it is known that the amino acids and mineral elements are important nutritional components of tea, and so by measuring their compositions and contents, we can establish an improved understanding of the different characteristics of teas and provide support for the rational development and utilization of tea as a nutritional health food.

3.1.2. Physicochemical properties

The majority of plant-derived dietary fiber is classified as IDF, which contains functional groups such as phenols, carboxylic acids, aldehydes, ketones, and ethers (Elleuch et al., 2011). These groups have a strong affinity for water, oil, or toxic metal ions. As shown in Table 2, the WHC, OHC, SC and CEC of T-IDF were 4.35 ± 0.03 g/g, 2.18 ± 0.03 g/g, 2.03 ± 0.04 mL/g, and 0.28 ± 0.02 mmol/g, respectively. In addition, the CAC of T-IDF at pH 2.0 and 7.0 were 2.0 ± 0.09 and 4.3 ± 0.02 mg/g, respectively. These physicochemical properties allow T-IDF to moisten feces, improve intestinal peristalsis, increase the fecal volume, and remove heavy metals, oils, and other unnecessary substances to regulate the intestines (Hua et al., 2019). Our results also indicated that the WHC of T-IDF was higher than that of bamboo shoot IDF (2.83 g/g), while the OHC was higher than those of superfine rice bran IDF (1.72 g/g), and lotus root IDF (0.61–1.50 g/g) (Hussain, Li, Jin, Yan, & Wang, 2018). Furthermore, the ability of T-IDF to adsorb cholesterol at pH 7.0 was significantly higher than that at pH 2.0, thereby indicating that T-IDF may lower the concentration of cholesterol in the small intestine.

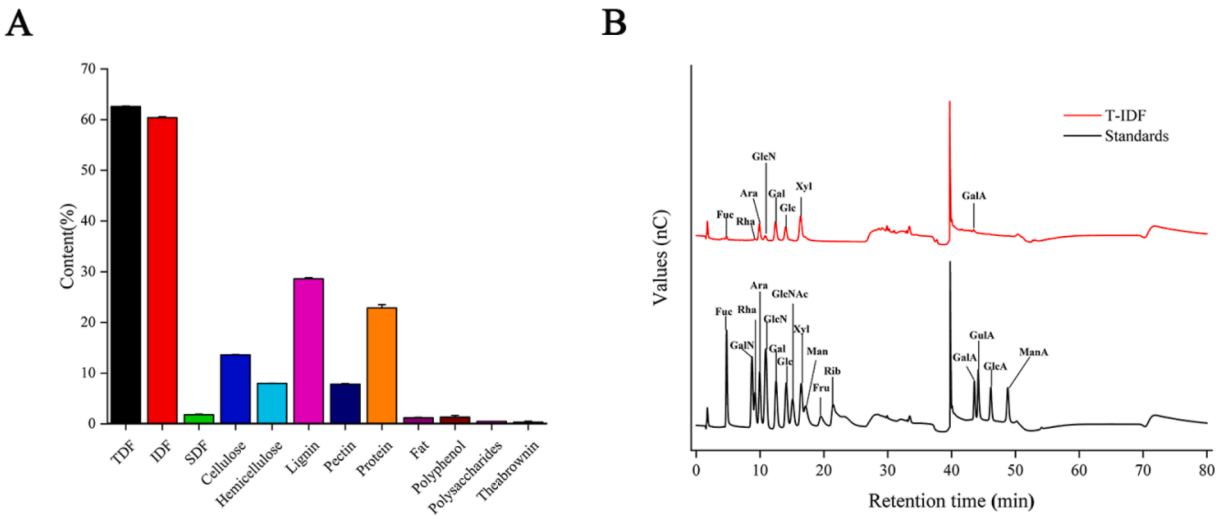

Fig. 1. Component analysis of T-IDF. (A) Basic component of T-IDF; (B) Monosaccharide chromatogram profile for T-IDF; Data are expressed as mean ± S.D. (n = 3). *The peaks at 2.0 and 40 min correspond to sodium hydroxide and sodium acetate, respectively.

Table 1
Amino acid and mineral element contents in T-IDF.

Amino acid contents(g/100 g)		Mineral elements (%)	
EAAs		N	3.48
Thr	0.98	P	0.14
Val	1.00	K	0.088
Met	0.11	Mineral elements (mg/kg dry weight)	
Ile	0.97	Na	3.6×10^2
Leu	1.83	Mg	1.6×10^3
Trp	3.07	Al	1.2×10^3
Phe	1.16	Ca	1.0×10^4
Lys	1.88	Cr	3.0
NEAAs		Mn	6.4×10^2
L-Cys	0.09	Fe	5.5×10^2
Asp	2.11	Ni	3.0
Glu	2.59	Cu	26
Ser	1.18	Zn	31
Arg	1.04	As	0.18
Gly	1.22	Se	0.050
Pro	1.09	Cd	0.062
Ala	1.40	Hg	0.28
Cys	0.07	Pb	1.2
His	0.51	TMs	5.15×10^4
Tyr	0.92		
Total EAA (TEAA)	11.00		
Total NEAA (TNEAA)	12.24		
TAAs	23.24		
TEAA/TNEAA	0.90		
TEAA/TAA	0.47		
Hydrophobic amino acid	10.63		

EAAs: essential amino acids; NEAAs: non-essential amino acids; TAAs: total amino acids; TMs: total minerals.

Table 2
Physicochemical properties of T-IDF.

Index	Content	SD
WHC (g/g)	4.35	0.03
OHC (g/g)	2.18	0.03
SC (mL/g)	2.03	0.04
CEC (mmol/g)	0.28	0.02
CAC (mg/g, pH 2.0)	2.0	0.09
CAC (mg/g, pH 7.0)	4.3	0.02

3.1.3. *Structural analysis*

IDF is usually composed of ordered carbon chains. When the polymer chains are intertwined to form a network structure, viscosity is generated. The chain length, molecular weight, particle size, and the type of side chain functional groups will therefore affect the physical and chemical properties of the resulting fiber, including its solubility, viscosity, fermentation, and physiological function (Ishisono, Mano, Yabe, & Kitaguchi, 2019).

Thus, the micro-structure of T-IDF was analyzed by SEM (Fig. 2A and 2B), and it was found that the T-IDF presented a loose, porous, wrinkled surface with a loose crack structure, which increased the contact area with water molecules.

XRD was then used to determine the structure and type of cellulose crystals present in T-IDF. As shown in Fig. 2C, T-IDF exhibited a cellulose I crystal structure with four conspicuous diffraction peaks of $2\theta = 15.19$, 22.22, 26.92, and 36.80°, suggesting the presence of a crystalline cellulose region. Using the Scherrer formula (Yalcin et al., 2015), the crystallinity of T-IDF was calculated to be 25.98 %.

Subsequently, the polysaccharide functional groups of T-IDF were revealed by FT-IR. As shown in Fig. 2D, the absorption at 3268 cm^{-1} is caused by the hydrogen bond stretching vibration, while the absorption at 2920 cm^{-1} was mainly attributed to the stretching vibration of the C—H bonds of the $–CH_3$ and $–CH_2$ groups, which are present in the typical structures of cellulose polysaccharide compounds (Kouadri & Satha, 2018). In addition, the prominent absorption peak at 1651 cm^{-1} was mainly due to the presence of ester groups and the ionized carboxyl group of galacturonic acid, while those at 1513 and 1444 cm^{-1} correlated with the vibrations of the aliphatic and/or aromatic C—H groups of lignin. Furthermore, the weak peak at 1374 cm^{-1} was mainly attributed to the typical cellulose structure, the weak peak at 1285 cm^{-1} originated from the O—H and/or C—O group vibrations of hemicellulose, and the peak at 1039 cm^{-1} corresponding to the C—O stretching vibration peak of the C—O—C bond, which is a typical absorption peak of xylan. These results therefore indicate that the T-IDF component contained xylanoid hemicelluloids (Esteves et al., 2013). Moreover, the small peak at 898 cm^{-1} was attributed to the bending vibration peak of C—H, which likely originates from the β-pyran ring. Indeed, the symmetrical stretching vibration of the D-botrytis pyran ring appeared at 775 cm^{-1}, thereby indicating that T-IDF contains a pyran-based structure. The variable angle vibration absorption peak of the C—H axial bond of the β-type sugar molecule is also clearly visible at 600 cm^{-1} (Belanche, Weisbjerg, Allison, Newbold, & Moorby, 2014).

Overall, these analytical results indicate that T-IDF contained the

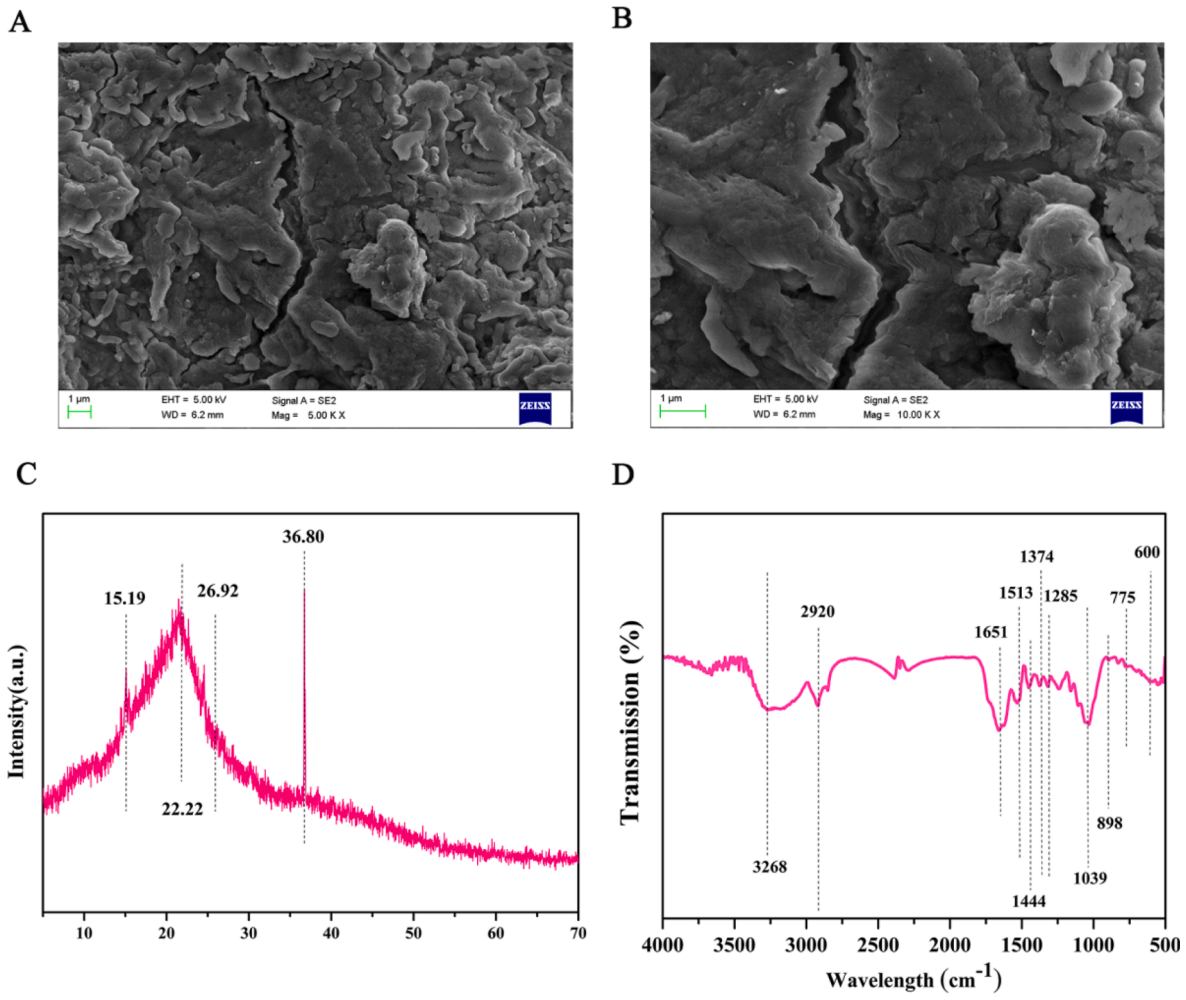

Fig. 2. Structural analysis of T-IDF. (A) and (B) SEM images of T-IDF; (C) XRD patterns and (D) FT-IR spectrum of T-IDF.

typical cellulose polysaccharide functional groups, including cellulose, hemicellulose, and lignin.

3.2. Ameliorative effect on slow transit constipation

As shown in Fig. 3, the ink pushing rate of the model group was significantly lower than that of the normal group ($p < 0.01$). In addition, the first defecation time, fecal weight, and particle number of the model group after 6 h were significantly lower than those in the normal group ($p < 0.01$), indicating that the STC mouse model was successfully established by the administration of diphenoxylate. As shown in Fig. 3A, the ink pushing rate of the T-IDF group increased by 9.97–25.23 %. Importantly, the T-IDF high-dose group showed significant differences from the model group ($p < 0.05$), while the T-IDF middle-dose group showed extremely significant differences compared with the model group ($p < 0.01$). Furthermore, we found that the first dejection time of the T-IDF group was shortened by 2.56–20.29 % (Fig. 3B), and the dejection time of the T-IDF low-dose group was significantly different from that of the model group ($p < 0.05$). It was also determined that the fecal weight of the T-IDF group was higher than that of the model group, which increased by 1.14–24.86 % (Fig. 3C). There was a significant difference between the T-IDF middle-dose group and the model group ($p < 0.05$), and the grain numbers recorded for the T-IDF groups were higher than that of the model group, which increased by 26.13–71.08 % (Fig. 3D). Furthermore, significant differences were observed between the T-IDF low-dose group and the model group ($p < 0.05$), and highly significant differences were found between the T-IDF high-dose group and the T-IDF middle-dose group compared with the model group ($p < 0.01$). These results therefore indicate that T-IDF has an obvious function in improving defecation; according to the evaluation standard of the animal defecation experiment, the effects of T-IDF on STC were positive (Liu, Chen, Yan, Li, & Jiang, 2019).

The weights of the mice in each group were also measured during the test (Fig. 3E and 3F). At the end of the test, the body weights of the mice in each T-IDF dosage group were lower than those in the model group. More specifically, the weight loss of mice in the T-IDF dose group ranged from 6.64 to 7.76 %, and there were significant difference between the T-IDF high-dose group and the model group ($p < 0.05$). Similarly, there were significant differences between the T-IDF middle-dose group and the model group ($p < 0.05$), and there were extremely significant differences between the T-IDF low-dose group and the model group ($p < 0.01$). The weight loss effect of T-IDF may therefore be attributed to the fact that T-IDF is a non-digestible substance, and so it can reduce food intake, delay gastric emptying, and increase satiety by filling the stomach (Ratanpaul et al., 2021). In addition, T-IDF absorbs fat, which can reduce the intestinal absorption of fat, promote fat excretion, and prevent excess heat and fat accumulation, thereby achieving weight loss and weight regulation (Liu et al., 2021).

The digestion process that takes place in the gastrointestinal tract loosens the binding between proteins and dietary fiber, thereby allowing for a greater utilization of protein for enteral nutrition. This largely determines the fermentation degree of dietary fiber in the intestinal tract and affects its physiological function. Dietary fiber and proteins are particularly important nutrients, and they have their own unique

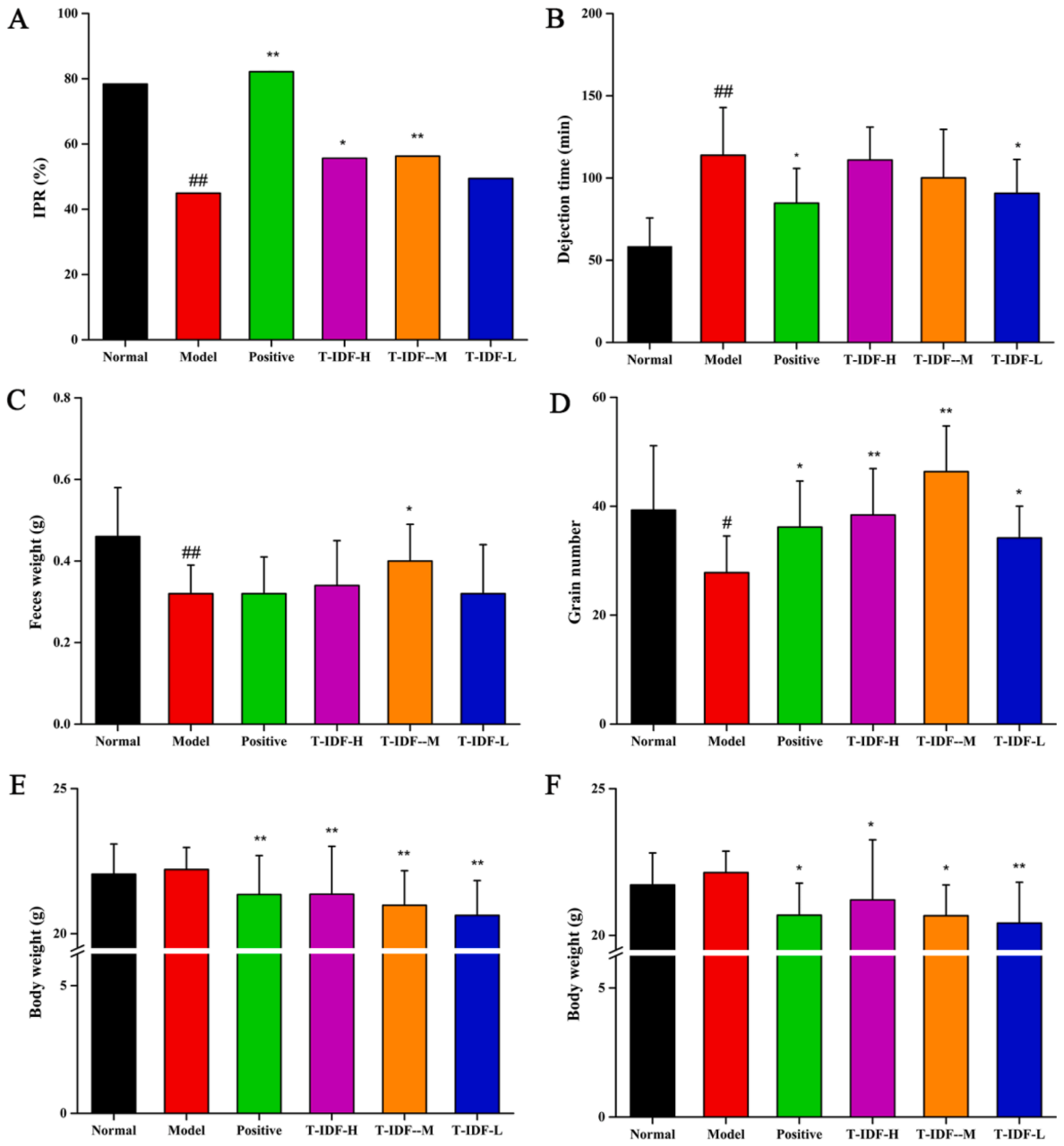

Fig. 3. Laxative effects of T-IDF on slow-transit constipation. (A) Ink pushing rate; (B) Defecation time (effects of T-IDF on defecation characteristics in constipation mice); (C) Feces weight, (D) Grain number (effect of T-IDF on body weight of STC mice during small intestine movement test); (E) 1 week and (F) 2 weeks (effect of T-IDF on body weight of STC mice) Data are expressed as mean ± S.D. (n = 10). #$p < 0.05$, ##$p < 0.01$ versus Normal group, *$p < 0.05$, **$p < 0.01$ versus Model group.

physiological activities. Ensuring the presence of appropriate proportions of dietary fiber and proteins may therefore prevent constipation to some degree; however, the synergistic effects between dietary fiber and proteins require further investigation.

3.3. *In vitro fermentation of T-IDF*

We note that this study confirmed the defecation function of T-IDF through mouse experiments. On this basis, in vitro simulation technology was used to simulate the for the human intestinal flora and study the intestinal microbial diversity and related functions. This approach is advantageous due to its convenient operation and good repeatability. The bacterial metabolism can therefore be inferred by measuring the content of short chain fatty acids present in the fermentation broth.

Thus, based on the above approach, we explored SCFA production in human feces during the *in vitro* fermentation of T-IDF as a preliminary step toward understanding the effects of T-IDF consumption by humans. As shown in Fig. 4, the concentration of SCFAs increased with fermentation time, and the production of SCFAs in the T-IDF groups was significantly higher than that in the control group after 8–12 h fermentation. Acetic acid was found to be the predominant SCFA during fermentation (from 0.30 ± 0.02 to 5.18 ± 1.07 mg/mL), followed by propionic acid (from 0.10 ± 0.03 to 0.47 ± 0.02 mg/mL), formic acid (from 0.12 ± 0.03 to 0.18 ± 0.02 mg/mL), and *n*-butyrate (from 0.08 ± 0.003 to 0.18 ± 0.03 mg/mL). The levels of SCFAs in the T-IDF groups were also significantly higher than that of the control group, and a 2 % T-IDF ingestion dose appeared to be the optimum level to produce SCFAs. These observations therefore suggested that T-IDF can enhance

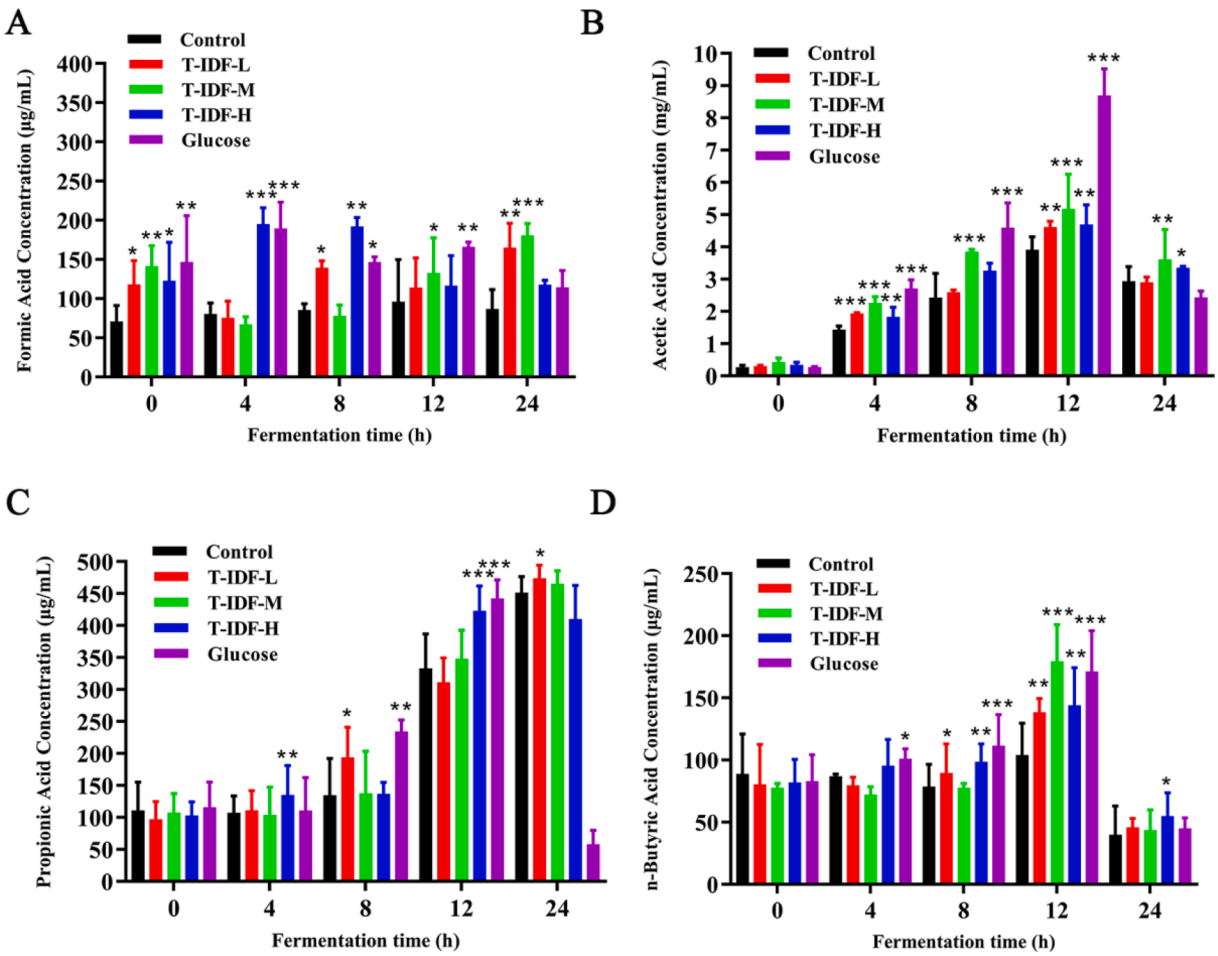

Fig. 4. The production of SCFAs after in vitro fermentation of T-IDF. $^{*}p < 0.05$, $^{**}p < 0.01$, $^{***}p < 0.001$ versus the control group. Data are expressed as mean ± S.D. (n = 3).

the production of SCFAs in the human colon.

Based on the above experiments, we speculated that T-IDF gradually improved the intestinal motility *via* two key processes: (1) T-IDF can increase the fecal weight, shorten the residence time of feces, and stimulate intestinal motility (de Vries, Birkett, Hulshof, Verbeke, & Gibes, 2016); and (2) T-IDF can be fermented by microorganisms in the gastrointestinal tract to produce SCFAs, which regulate colonic motion and accelerate colonic transport by regulating the release of polypeptides from pheochromocytoma cells and stimulating the release of 5-HT3 receptors on the sensory fibers of the vagus nerve (Fukumoto et al., 2003).

4. Conclusion

This study systematically studied the chemical composition, physical properties, chemical properties, and structure of T-IDF, in addition to evaluating its defecation effect on a slow transit constipation mouse model, and its in vitro fermentation behavior. Our results showed that the composition of T-IDF is reasonable, and that it exhibits good physical and chemical properties. In addition, we demonstrated that the consumption of T-IDF can improve intestinal function by increasing the weight and volume of feces through binding to water molecules, stimulating the intestinal wall to cause defecation, and accelerating intestinal peristalsis. Furthermore, the intestinal flora were demonstrated to ferment T-IDF to produce short-chain fatty acids, which can regulate the intestinal ecological environment. In the future research, it is necessary to further investigate the physiological function and action mechanism of T-IDF, in addition to developing a series of functional products rich in this substance, and improving its social and economic benefits.

Declaration of Competing Interest

The authors declare that they have no known competing financial interests or personal relationships that could have appeared to influence the work reported in this paper.

Acknowledgments

Financial supports from National Natural Science Foundation of China (32072203), Tianjin Synthetic Biotechnology Innovation Capacity Improvement Project (TSBICIP-KJGG-016-03), Tianjin Science and Technology Commission (21ZYJDJC00030), and Tianjin Municipal Education Commission (TD13-5013).

Ethical approval

This article does not contain any studies with human subjects. All animal studies were carried out under the guidance of the animal welfare committee of Nankai University.

References

Belanche, A., Weisbjerg, M. R., Allison, G. G., Newbold, C. J., & Moorby, J. M. (2014). Measurement of rumen dry matter and neutral detergent fiber degradability of feeds by Fourier-transform infrared spectroscopy. *Journal of Dairy Science, 97*(4), 2361–2375. https://doi.org/10.3168/jds.2013-7491

Benitez, V., Molla, E., Martin-Cabrejas, M., Aguilera, Y., & Esteban, R. M. (2017). Physicochemical properties and in vitro antidiabetic potential of fibre concentrates from onion by-products. *Journal of Functional Foods, 36*, 34–42. https://doi.org/10.1016/j.jff.2017.06.045

Bishehsari, F., Engen, P. A., Preite, N. Z., Tuncil, Y. E., Naqib, A., Shaikh, M., … Keshavarzian, A. (2018). Dietary fiber treatment corrects the composition of gut microbiota, promotes SCFA production, and suppresses colon carcinogenesis. *Genes, 9*(2), 17. https://doi.org/10.3390/genes9020102

Breynaert, A., Bosscher, D., Kahnt, A., Claeys, M., Cos, P., Pieters, L., & Hermans, N. (2015). Development and Validation of an in vitro Experimental GastroIntestinal Dialysis Model with Colon Phase to Study the Availability and Colonic Metabolisation of Polyphenolic Compounds. *Planta Med, 81*(12–13), 1075–1083. https://doi.org/10.1055/s-0035-1546154

Cuesta, G., Suarez, N., Bessio, M. I., Ferreira, F., & Massaldi, H. (2003). Quantitative determination of pneumococcal capsular polysaccharide serotype 14 using a modification of phenol-sulfuric acid method. *Journal of Microbiological Methods, 52*(1), 69–73. https://doi.org/10.1016/s0167-7012(02)00151-3

De Vries, J., Birkett, A., Hulshof, T., Verbeke, K., & Gibes, K. (2016). Effects of cereal, fruit and vegetable fibers on human fecal weight and transit time: A comprehensive review of intervention trials. *Nutrients, 8*(3), 10. https://doi.org/10.3390/nu8030130

Elleuch, M., Bedigian, D., Roiseux, O., Besbes, S., Blecker, C., & Attia, H. (2011). Dietary fibre and fibre-rich by-products of food processing: Characterisation, technological functionality and commercial applications: A review. *Food Chemistry, 124*(2), 411–421. https://doi.org/10.1016/j.foodchem.2010.06.077

Esteves, B., Velez Marques, A., Domingos, I., & Pereira, H. (2013). Chemical changes of heat treated pine and eucalypt wood monitored by FTIR. *Maderas-Ciencia Y Tecnologia, 15*(2), 245–258. https://doi.org/10.4067/s0718-221x2013005000020

FAO. (2018). Global tea consumption and production driven by robust demand in China and India. Retrieved from http://www.fao.org/ news/story/en/item/1136255/icode/.

Fukumoto, S., Tatewaki, M., Yamada, T., Fujimiya, M., Mantyh, C., Voss, M., … Takahashi, T. (2003). Short-chain fatty acids stimulate colonic transit via intraluminal 5-HT release in rats. *American Journal of Physiology-Regulatory Integrative and Comparative Physiology, 284*(5), R1269–R1276. https://doi.org/10.1152/ajpregu.00442.2002

Hua, M., Lu, J., Qu, D., Liu, C., Zhang, L., Li, S., … Sun, Y. (2019). Structure, physicochemical properties and adsorption function of insoluble dietary fiber from ginseng residue: A potential functional ingredient. *Food Chemistry, 286*(JUL.15), 522–529. https://doi.org/10.1016/j.foodchem.2019.01.114

Hussain, S., Li, J., Jin, W. J., Yan, S. L., & Wang, Q. Z. (2018). Effect of micronisation on dietary fibre content and hydration properties of lotus node powder fractions. *International Journal of Food Science and Technology, 53*(3), 590–598. https://doi.org/10.1111/ijfs.13632

Ishisono, K., Mano, T., Yabe, T., & Kitaguchi, K. (2019). Dietary Fiber Pectin Ameliorates Experimental Colitis in a Neutral Sugar Side Chain-Dependent Manner. *Front Immunol, 10*, 2979. https://doi.org/10.3389/fimmu.2019.02979

Kouadri, I., & Satha, H. (2018). Extraction and characterization of cellulose and cellulose nanofibers from Citrullus colocynthis seeds. *Industrial Crops and Products, 124*, 787–796. https://doi.org/10.1016/j.indcrop.2018.08.051

Li, N., Liu, Y., Zhao, Y., Zheng, X., Lu, J., & Liang, Y. (2016). Simultaneous HPLC Determination of Amino Acids in Tea Infusion Coupled to Pre-column Derivatization with 2,4-Dinitrofluorobenzene. *Food Analytical Methods, 9*(5), 1307–1314. https://doi.org/10.1007/s12161-015-0310-8

Liu, Q., Zhao, J. Y., Liu, S. S., Fan, Y. C., Mei, J. J., Liu, X. J., & Wei, T. (2021). Positive intervention of insoluble dietary fiber from defatted rice bran on hyperlipidemia in high fat diet fed rats. *Journal of Food Science, 86*(9), 3964–3974. https://doi.org/10.1111/1750-3841.15812

Liu, X., Chen, S., Yan, Q., Li, Y., & Jiang, Z. (2019). Effect of Konjac mannan oligosaccharides on diphenoxylate-induced constipation in mice. *Journal of Functional Foods, 57*(C), 399–407. https://doi.org/10.1016/j.jff.2019.04.036

Luo, X., Wang, Q., Zheng, B., Lin, L., Chen, B., Zheng, Y., & Xiao, J. (2017). Hydration properties and binding capacities of dietary fibers from bamboo shoot shell and its hypolipidemic effects in mice. *Food and chemical toxicology, 109*, 1003–1009. https://doi.org/10.1016/j.fct.2017.02.029

Ratanpaul, V., Zhang, D. G., Williams, B. A., Diffey, S., Black, J. L., & Gidley, M. J. (2021). Interplay between grain digestion and fibre in relation to gastro-small-intestinal passage rate and feed intake in pigs. *European Journal of Nutrition, 60*(7), 4001–4017. https://doi.org/10.1007/s00394-021-02567-3

Reynolds, A., Mann, J., Cummings, J. H., Winter, N., Mete, E., & Te Morenga, L. (2019). Carbohydrate quality and human health: A series of systematic reviews and meta-analyses. *Lancet, 393*(10170), 434–445. https://doi.org/10.1016/s0140-6736(18)31809-9

Ritz, N. L., Lin, D. M., Wilson, M. R., Barton, L. L., & Lin, H. C. (2017). Sulfate-reducing bacteria slow intestinal transit in a bismuth-reversible fashion in mice. *Neurogastroenterology and Motility, 29*(1), e12907.

Robertson, G. L. (1979). The fractional extraction and quantitative determination of pectic substances in grapes and musts. *American Journal Of Enology & Viticulture.*

Mugie, S. M., Benninga, M. A., & Di Lorenzo, C. (2011). Epidemiology of constipation in children and adults: A systematic review. *Best Practice & Research Clinical Gastroenterology, 25*(1), 3–18. https://doi.org/10.1016/j.bpg.2010.12.010

Sacranie, A., Svihus, B., Denstadli, V., Moen, B., Iji, P. A., & Choct, M. (2012). The effect of insoluble fiber and intermittent feeding on gizzard development, gut motility, and performance of broiler chickens. *Poultry Science, 91*(3), 693–700. https://doi.org/10.3382/ps.2011-01790

Tadesse, E., Engidawork, E., Nedi, T., & Mengistu, G. (2017). Evaluation of the anti-diarrheal activity of the aqueous stem extract of Lantana camara Linn (Verbenaceae) in mice. *Bmc Complementary and Alternative Medicine, 17*(1), 1–8. https://doi.org/10.1186/s12906-017-1696-1

Temtrirath, K. (2022). A uhplc-pda method for the quantitative analysis of total amino acids in infant formula with microwave-assisted acid hydrolysis. *Chemical Papers, 76*(5), 3065–3076. https://doi.org/10.1007/s11696-022-02078-3

Tsubaki, S., & Azuma, J. (2013). Total fractionation of green tea residue by microwave-assisted alkaline pretreatment and enzymatic hydrolysis. *Bioresource Technology, 131*, 485–491. https://doi.org/10.1016/j.biortech.2013.01.001

Van Soest, P. J., Robertson, J. B., & Lewis, B. A. (1991). Methods for dietary fiber, neutral detergent fiber, and nonstarch polysaccharides in relation to animal nutrition. *Journal of dairy science, 74*(10), 3583–3597. https://doi.org/10.3168/jds.S0022-0302(91)78551-2

Waterhouse, A. L. (2003). Determination of total phenolics. *Current Protocols In Foodanalytical Chemistry*. https://doi.org/10.1002/0471142913.fai0101s06

Yalcin, S., Khodadust, R., Unsoy, G., Garip, I. C., Mumcuoglu, Z. D., & Gunduz, U. (2015). Synthesis and characterization of polyhydroxybutyrate coated magnetic nanoparticles: toxicity analyses on different cell lines. *Synthesis and Reactivity in Inorganic Metal-Organic and Nano-Metal Chemistry, 45*(5), 700–708. https://doi.org/10.1080/15533174.2013.831448

Zhang, W. M., Zeng, G. L., Pan, Y. G., Chen, W. X., Huang, W. Y., Chen, H. M., & Li, Y. S. (2017). Properties of soluble dietary fiber-polysaccharide from papaya peel obtained through alkaline or ultrasound-assisted alkaline extraction. *Carbohydrate Polymers, 172*, 102–112. https://doi.org/10.1016/j.carbpol.2017.05.030

Zhang, X. Y., Tian, H. L., Gu, L. L., Nie, Y. Z., Ding, C., Ge, X. L., … Li, N. (2018). Long-term follow-up of the effects of fecal microbiota transplantation in combination with soluble dietary fiber as a therapeutic regimen in slow transit constipation. *Science China-Life Sciences, 61*(7), 779–786. https://doi.org/10.1007/s11427-017-9229-1

Zhao, G. H., Nyman, M., & Jonsson, J. A. (2006). Rapid determination of short-chain fatty acids in colonic contents and faeces of humans and rats by acidified water-extraction and direct-injection gas chromatography. *Biomedical Chromatography, 20*(8), 674–682. https://doi.org/10.1002/bmc.580